# NONLINEAR VIBRATIONS OF FUNCTIONALLY GRADED CYLINDRICAL SHELLS: EFFECT OF THE COMPANION MODE PARTICIPATION

Angelo Oreste Andrisano
*Department of Engineering "Enzo Ferrari", University of Modena and Reggio Emilia, Italy*
*E-mail: angelooreste.andrisano@unimore.it*

Francesco Pellicano
*Department of Engineering "Enzo Ferrari", University of Modena and Reggio Emilia, Italy*
*E-mail: francesco.pellicano@unimore.it*

Matteo Strozzi
*Department of Engineering "Enzo Ferrari", University of Modena and Reggio Emilia, Italy*
*E-mail: matteo.strozzi@unimore.it*

**Abstract**. *In this paper, the effect of the companion mode participation on the nonlinear vibrations of functionally graded (FGM) cylindrical shells is analysed. The Sanders-Koiter theory is applied to model the nonlinear dynamics of the system in the case of finite amplitude of vibration. The shell deformation is described in terms of longitudinal, circumferential and radial displacement fields. Simply supported boundary conditions are considered. The displacement fields are expanded by means of a double mixed series based on Chebyshev polynomials for the longitudinal variable and harmonic functions for the circumferential variable. Both driven and companion modes are considered. Numerical analyses are carried out in order to characterize the nonlinear response when the shell is subjected to a harmonic external load. A convergence analysis is carried out considering a different number of axisymmetric and asymmetric modes. The present study is focused on modelling the nonlinear travelling-wave response of the FGM shell in the circumferential direction with the companion mode participation.*

***Keywords****: functionally graded, cylindrical shells, nonlinear vibrations*

## 1. INTRODUCTION

Functionally graded materials (FGMs) are composite materials obtained by combining and mixing two or more different constituent materials, which are distributed along the thickness in accordance with a volume fraction law. Most of the FGMs are employed in the high-temperature environments because of their heat shielding capacity.

The idea of FGMs was first introduced in 1984/87 by a group of Japanese material scientists [1]. They studied many different physical aspects such as temperature and thermal stress distributions, static and dynamic responses.

Loy et al. [2] analysed the vibrations of the circular cylindrical shells made of FGM, considering simply supported boundary conditions. They found that the natural frequencies are affected by the constituent volume fractions and configurations of the materials.

Pradhan et al. [3] studied the vibration characteristics of FGM cylindrical shells made of stainless steel and zirconia, under different boundary conditions. They found that the natural frequencies depend on the material distributions and boundary conditions.

Leissa [4] analysed the linear dynamics of shells having different topologies, materials and boundary conditions, considering the most important shell theories, such as Donnell, Flugge and Sanders-Koiter.

Yamaki [5] studied buckling and post-buckling of the shells in the linear and nonlinear field, reporting the solution methods, numerical and experimental results.

A modern treatise on the shells dynamics and stability can be found in Ref. [6], where also FGMs are considered.

Pellicano et al. [7] considered the nonlinear vibrations of homogeneous isotropic shells, leading to similar conclusions of the present work.

The method of solution used in the present work was presented in Ref. [8].

In the present paper, the effect of the companion mode participation on the nonlinear vibrations of FGM circular cylindrical shells is analysed.

The Sanders-Koiter theory is applied to model the nonlinear dynamics of the system in the case of finite amplitude of vibration.

The shell deformation is described in terms of longitudinal, circumferential and radial displacement fields.

Simply supported boundary conditions are considered.

The FGM is made of a uniform distribution of stainless steel and nickel, and the material properties are graded in the thickness direction, according to a volume fraction power-law distribution.

The solution method consists of two steps:

1) linear analysis and eigenfunctions evaluation;

2) nonlinear analysis, using an eigenfunction based expansion.

In the linear analysis, the displacement fields are expanded by means of a double series based on harmonic functions for the circumferential variable and Chebyshev polynomials for the longitudinal variable.

A Ritz based method allows to obtain the approximate natural frequencies and mode shapes (eigenvalues and eigenvectors).

In the nonlinear analysis, the three displacement fields are re-expanded by using the approximate eigenfunctions. Both driven and companion modes are considered.

An energy approach based on the Lagrange equations is then considered, in order to reduce the nonlinear partial differential equations to a set of nonlinear ordinary differential equations.

Numerical analyses are carried out in order to characterize the nonlinear response when the shell is subjected to a harmonic external load.

A convergence analysis is carried out on a simply supported cylindrical shell to obtain the correct number of axisymmetric and asymmetric modes able to describe the actual nonlinear behaviour of the shell. Comparisons of nonlinear amplitude-frequency curves of the cylindrical shell with different nonlinear expansions are carried out.

The influence of the companion mode participation on the nonlinear response of the shell is analysed. The nonlinear travelling-wave response of the shell in the circumferential direction with the companion mode participation is modelled.

## 2. FUNCTIONALLY GRADED MATERIALS

A generic material property $P_{fgm}$ of an FGM depends on the material properties and the volume fractions of the constituent materials, and it is expressed in the form [2]

$$P_{fgm}(T,z) = \sum_{i=1}^{k} \widetilde{P}_i(T) V_{fi}(z) \tag{1}$$

where $\widetilde{P}_i$ and $V_{fi}$ are the material property and volume fraction of the constituent material $i$, respectively.

The material property $\widetilde{P}_i$ of a constituent material can be described as a function of the environmental temperature $T$(K) by Touloukian's relation [2] (the index $i$ is dropped for the sake of simplicity)

$$\tilde{P}(T) = P_0(P_{-1}T^{-1} + 1 + P_1T + P_2T^2 + P_3T^3) \tag{2}$$

where $P_0$, $P_{-1}$, $P_1$, $P_2$ and $P_3$ are the coefficients of temperature of the constituent material.

In the case of an FGM thin cylindrical shell with a uniform thickness $h$ and a reference surface at its middle surface, the volume fraction $V_f$ of a constituent material can be written as [2]

$$V_f(z) = \left(\frac{z + h/2}{h}\right)^p \tag{3}$$

where the power-law exponent $p$ is a positive real number, $(0 \le p \le \infty)$, and $z$ describes the radial distance measured from the middle surface of the shell, $(-h/2 \le z \le h/2)$, as shown in Fig. 1.

For an FGM thin cylindrical shell made of two different constituent materials 1 and 2, the volume fractions $V_{f1}$ and $V_{f2}$ can be written in the following form [3]

$$V_{f1}(z) = 1 - \left(\frac{z + h/2}{h}\right)^p \qquad V_{f2}(z) = \left(\frac{z + h/2}{h}\right)^p \qquad V_{f1}(z) + V_{f2}(z) = 1 \tag{4}$$

where the sum of the volume fractions of the constituent materials is equal to unity.

Young's modulus $E$, Poisson's ratio $\nu$ and mass density $\rho$ are expressed as [3]

$$E_{fgm}(T,z) = \big(E_2(T) - E_1(T)\big)\left(\frac{z + h/2}{h}\right)^p + E_1(T) \tag{5}$$

$$\nu_{fgm}(T,z) = \big(\nu_2(T) - \nu_1(T)\big)\left(\frac{z + h/2}{h}\right)^p + \nu_1(T) \tag{6}$$

$$\rho_{fgm}(T,z) = \big(\rho_2(T) - \rho_1(T)\big)\left(\frac{z + h/2}{h}\right)^p + \rho_1(T) \tag{7}$$

## 3. SANDERS-KOITER THEORY

In Figure 1, an FGM circular cylindrical shell having radius $R$, length $L$ and thickness $h$ is represented; a cylindrical coordinate system $(O; x, \theta, z)$ is considered in order to take advantage from the axial symmetry of the structure, the origin $O$ of the reference system is located at the centre of one end of the shell. Three displacement fields are represented in Fig. 1: longitudinal $u(x, \theta, t)$, circumferential $v(x, \theta, t)$ and radial $w(x, \theta, t)$.

**Elastic Strain Energy, Kinetic Energy, Virtual Work, Damping Forces**

The Sanders-Koiter nonlinear theory of circular cylindrical shells, which is an eight-order shell theory, is based on the Love's "first approximation" [4]. The strain components $(\varepsilon_x, \varepsilon_\theta, \gamma_{x\theta})$ at an arbitrary point of the shell are related to the middle surface strains $(\varepsilon_{x,0}, \varepsilon_{\theta,0}, \gamma_{x\theta,0})$ and to the changes in the curvature and torsion $(k_x, k_\theta, k_{x\theta})$ of the middle surface of the shell by the following relationships [5]

$$\varepsilon_x = \varepsilon_{x,0} + zk_x \qquad \varepsilon_\theta = \varepsilon_{\theta,0} + zk_\theta \qquad \gamma_{x\theta} = \gamma_{x\theta,0} + zk_{x\theta} \tag{8}$$

where $z$ is the distance of the arbitrary point of the cylindrical shell from the middle surface and $(x, \theta)$ are the longitudinal and angular coordinates of the shell, see Fig. 1.

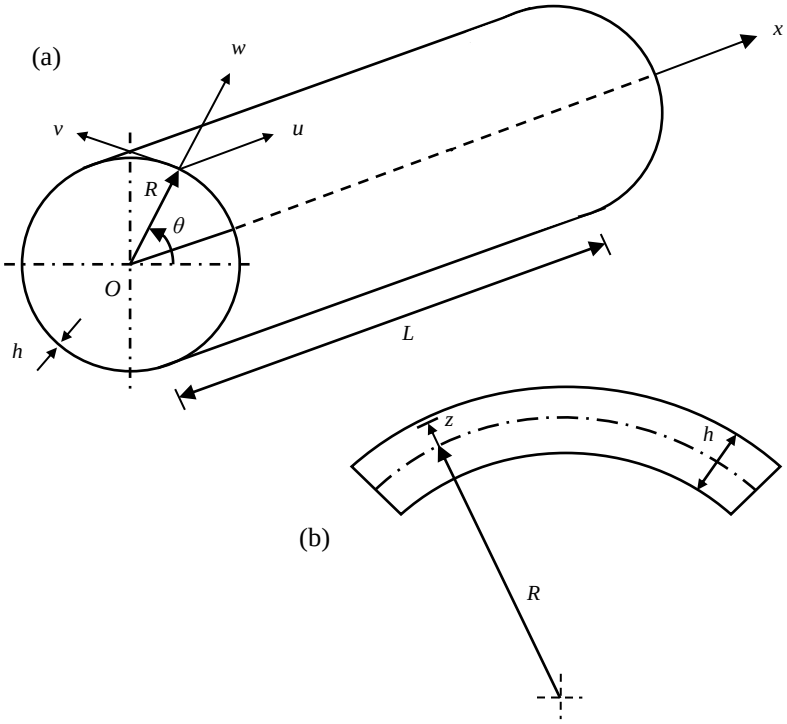


**Figure 1.** Geometry of the functionally graded cylindrical shell.
(a) Complete shell; (b) cross-section of the shell surface.

The middle surface strains and changes in curvature and torsion are given by [5]

$$\varepsilon_{x,0} = \frac{\partial u}{L\partial\eta} + \frac{1}{2}\left(\frac{\partial w}{L\partial\eta}\right)^2 + \frac{1}{8}\left(\frac{\partial v}{L\partial\eta} - \frac{\partial u}{R\partial\theta}\right)^2 + \frac{\partial w}{L\partial\eta}\frac{\partial w_0}{L\partial\eta}$$

$$\varepsilon_{\theta,0} = \frac{\partial v}{R\partial\theta} + \frac{w}{R} + \frac{1}{2}\left(\frac{\partial w}{R\partial\theta} - \frac{v}{R}\right)^2 + \frac{1}{8}\left(\frac{\partial u}{R\partial\theta} - \frac{\partial v}{L\partial\eta}\right)^2 + \frac{\partial w_0}{R\partial\theta}\left(\frac{\partial w}{R\partial\theta} - \frac{v}{R}\right)$$

$$\gamma_{x\theta,0} = \frac{\partial u}{R\partial\theta} + \frac{\partial v}{L\partial\eta} + \frac{\partial w}{L\partial\eta}\left(\frac{\partial w}{R\partial\theta} - \frac{v}{R}\right) + \frac{\partial w_0}{L\partial\eta}\left(\frac{\partial w}{R\partial\theta} - \frac{v}{R}\right) + \frac{\partial w}{L\partial\eta}\frac{\partial w_0}{R\partial\theta}$$

$$k_x = -\frac{\partial^2 w}{L^2\partial\eta^2} \quad k_\theta = \frac{\partial v}{R^2\partial\theta} - \frac{\partial^2 w}{R^2\partial\theta^2} \quad k_{x\theta} = -2\frac{\partial^2 w}{LR\partial\eta\partial\theta} + \frac{1}{2R}\left(3\frac{\partial v}{L\partial\eta} - \frac{\partial u}{R\partial\theta}\right) \quad (9)$$

where $(\eta = x/L)$ is the nondimensional longitudinal coordinate.

In the case of FGMs, the stresses are related to the strains as follows [6]

$$\sigma_x = \frac{E(z)}{1-\nu^2(z)}(\varepsilon_x + \nu(z)\varepsilon_\theta) \;\; \sigma_\theta = \frac{E(z)}{1-\nu^2(z)}(\varepsilon_\theta + \nu(z)\varepsilon_x) \;\; \tau_{x\theta} = \frac{E(z)}{2\left(1+\nu(z)\right)}\gamma_{x\theta} \quad (10)$$

where $E(z)$ is the Young's modulus and $\nu(z)$ is the Poisson's ratio ($\sigma_z = 0$, plane stress).

The elastic strain energy $U_s$ of a cylindrical shell is given by [6]

$$U_s = \frac{1}{2}LR\int_0^1\int_0^{2\pi}\int_{-h/2}^{h/2}(\sigma_x\varepsilon_x + \sigma_\theta\varepsilon_\theta + \tau_{x\theta}\gamma_{x\theta})\,d\eta d\theta dz \quad (11)$$

The kinetic energy $T_s$ of a cylindrical shell (rotary inertia effect is neglected) is given by [6]

$$T_s = \frac{1}{2}LR\int_0^1\int_0^{2\pi}\int_{-h/2}^{h/2}\rho(z)\,(\dot{u}^2 + \dot{v}^2 + \dot{w}^2)\,d\eta d\theta dz \quad (12)$$

where $\rho(z)$ is the mass density of the shell.

The virtual work $W$ done by the external forces is written as [6]

$$W = LR\int_0^1\int_0^{2\pi}(q_x u + q_\theta v + q_z w)d\eta d\theta \quad (13)$$

with $(q_x, q_\theta, q_z)$ as distributed forces in longitudinal, circumferential and radial direction.

The nonconservative damping forces are assumed to be of viscous type and are taken into account by using Rayleigh's dissipation function (viscous damping coefficient $c$) [6]

$$F = \frac{1}{2}cLR\int_0^{2\pi}\int_0^1(\dot{u}^2 + \dot{v}^2 + \dot{w}^2)\,d\eta d\theta \quad (14)$$

## 4. VIBRATION ANALYSIS

In order to carry out the dynamic analysis of the shell a two-steps procedure is considered [8]: *i*) the Rayleigh-Ritz method is applied to the linearized formulation of the problem, in order to obtain an approximation of the eigenfunctions; *ii*) the displacement fields are re-expanded using the approximate eigenfunctions, the Lagrange equations are considered in conjunction with the fully nonlinear expression of the potential energy, in order to obtain a set of nonlinear ordinary differential equations in modal coordinates.

### Linear Vibration Analysis: Discretization Approach

In order to carry out a linear vibration analysis only the quadratic terms are retained in Eqn. (11). A modal vibration, i.e. a synchronous motion, is obtained in the form [8]

$$u(\eta,\theta,t) = U(\eta,\theta)f(t) \qquad v(\eta,\theta,t) = V(\eta,\theta)f(t) \qquad w(\eta,\theta,t) = W(\eta,\theta)f(t) \tag{15}$$

where $u(\eta,\theta,t), v(\eta,\theta,t), w(\eta,\theta,t)$ are the displacement fields, $U(\eta,\theta)$, $V(\eta,\theta), W(\eta,\theta)$ represent the modal shape and $f(t)$ describes the time law, which is supposed to be the same for each displacement field (synchronous motion hypothesis).

The components of the modal shape are expanded by means of a double mixed series: the periodicity of deformation in the circumferential direction suggests the use of harmonic functions ($\cos n\theta$ , $\sin n\theta$), while Chebyshev orthogonal polynomials are considered in the longitudinal direction $T_m^*(\eta)$ [8]

$$U(\eta,\theta) = \sum_{m=0}^{M_u}\sum_{n=0}^{N} \tilde{U}_{m,n} T_m^*(\eta)\cos n\theta \qquad V(\eta,\theta) = \sum_{m=0}^{M_v}\sum_{n=0}^{N} \tilde{V}_{m,n} T_m^*(\eta) sin\, n\theta$$

$$W(\eta,\theta) = \sum_{m=0}^{M_w}\sum_{n=0}^{N} \tilde{W}_{m,n} T_m^*(\eta)\cos n\theta \tag{16}$$

where $T_m^*(\eta) = T_m(2\eta - 1)$, $m$ denotes the degree of the Chebyshev polynomials, $n$ is the number of nodal diameters and $\left(\tilde{U}_{m,n}, \tilde{V}_{m,n}, \tilde{W}_{m,n}\right)$ are the generalized coordinates.

### Boundary Conditions

Simply supported – simply supported (S – S) boundary conditions are given by [4]

$$w = 0 \qquad v = 0 \qquad M_x = 0 \qquad N_x = 0 \qquad \text{for} \quad \eta = 0,1 \tag{17}$$

The previous conditions imply the following equations [8]

$$\sum_{m=0}^{M_w} \tilde{W}_{m,n}\, T_m^*(\eta) = 0 \qquad \theta\epsilon[0,2\pi] \qquad n\epsilon[0,N] \qquad \text{for} \quad \eta = 0,1 \tag{18}$$

$$\sum_{m=0}^{M_v} \tilde{V}_{m,n}\, T_m^*(\eta) = 0 \qquad \theta\epsilon[0,2\pi] \qquad n\epsilon[0,N] \qquad \text{for} \quad \eta = 0,1 \qquad (19)$$

$$\sum_{m=0}^{M_w} \widetilde{W}_{m,n}\, T_{m,\eta\eta}^*(\eta) = 0 \qquad \theta\epsilon[0,2\pi] \qquad n\epsilon[0,N] \qquad \text{for} \quad \eta = 0,1 \qquad (20)$$

$$\sum_{m=0}^{M_u} \widetilde{U}_{m,n}\, T_{m,\eta}^*(\eta) = 0 \qquad \theta\epsilon[0,2\pi] \qquad n\epsilon[0,N] \qquad \text{for} \quad \eta = 0,1 \qquad (21)$$

The linear algebraic system given by Eqns. (17) can be solved analytically in terms of the coefficients $\left(\widetilde{U}_{1,n}, \widetilde{U}_{2,n}, \tilde{V}_{0,n}, \tilde{V}_{1,n}, \widetilde{W}_{0,n}, \widetilde{W}_{1,n}, \widetilde{W}_{2,n}, \widetilde{W}_{3,n}\right)$, for $n\epsilon[0,N]$.

**Rayleigh-Ritz Procedure**

The maximum number of variables needed for describing a generic vibration mode can be calculated by the relation $\left(N_p = M_u + M_v + M_w + 3 - r\right)$, with $(M_u = M_v = M_w)$ as the maximum degree of the Chebyshev polynomials and $r$ as the number of equations for the boundary conditions considered.

For a multi-mode analysis including different nodal diameters, the number of degrees of freedom of the system is computed by the relation $\left(N_{max} = N_p \times (N+1)\right)$, where $N$ describes the maximum number of nodal diameters considered.

Equations (15) are inserted in the expressions of $U_s$ and $T_s$ (Eqns. $(11-12)$).

Consider now the Rayleigh quotient $R(\tilde{\mathbf{q}}) = V_{max}/T^*$, where $V_{max}$ is the maximum of the potential energy, $T^* = T_{max}/\omega^2$, $T_{max}$ denotes the maximum of the kinetic energy, $\omega$ is the circular frequency of the harmonic motion and $\tilde{\mathbf{q}} = \left[\ldots, \widetilde{U}_{m,n}, \tilde{V}_{m,n}, \widetilde{W}_{m,n}, \ldots\right]^T$ denotes a vector containing all the unknowns.

After imposing the stationarity to the Rayleigh quotient, one obtains the eigenvalue problem [8]

$$(-\omega^2\mathbf{M} + \mathbf{K})\tilde{\mathbf{q}} = \mathbf{0} \qquad (22)$$

which furnishes natural frequencies and modes of vibration (eigenvalues and eigenvectors) of the system.

The modal shape is given by the Eqns. (16), where coefficients $(\widetilde{U}_{m,n}, \tilde{V}_{m,n}, \widetilde{W}_{m,n})$ are substituted with $(\widetilde{U}_{m,n}^{(j)}, \tilde{V}_{m,n}^{(j)}, \widetilde{W}_{m,n}^{(j)})$, which are the components of the j-th eigenvector $\tilde{\mathbf{q}}_j$ of the Eqn. (22).

The vector function $\boldsymbol{U}^{(j)}(\eta,\theta) = \left[U^{(j)}(\eta,\theta), V^{(j)}(\eta,\theta), W^{(j)}(\eta,\theta)\right]^T$ represents an approximation of the j-th mode of the original problem.

The eigenfunctions obtained are eventually normalized by imposing the following relation [8]

$$max\left[max\left[U^{(j)}(\eta,\theta)\right], max\left[V^{(j)}(\eta,\theta)\right], max\left[W^{(j)}(\eta,\theta)\right]\right] = 1 \qquad (23)$$

**Nonlinear Vibration Analysis: Lagrange Equations**

In the nonlinear vibration analysis, the full expression of the elastic strain energy (11), containing terms up to the fourth order (cubic nonlinearity), is considered.

The displacement fields $u(\eta,\theta,t), v(\eta,\theta,t), w(\eta,\theta,t)$ are expanded by using both the linear mode shapes $U(\eta,\theta), V(\eta,\theta), W(\eta,\theta)$, obtained in the previous linear analysis, and the conjugate mode shapes $U_c(\eta,\theta), V_c(\eta,\theta), W_c(\eta,\theta)$, in the following form [8]

$$u(\eta,\theta,t) = \sum_{j=1}^{N_u}\sum_{n=1}^{N}\left[U^{(j,n)}(\eta,\theta) f_{u,j,n}(t) + U_c{}^{(j,n)}(\eta,\theta) f_{u,j,n,c}(t)\right]$$

$$v(\eta,\theta,t) = \sum_{j=1}^{N_v}\sum_{n=1}^{N}\left[V^{(j,n)}(\eta,\theta) f_{v,j,n}(t) + V_c{}^{(j,n)}(\eta,\theta) f_{v,j,n,c}(t)\right]$$

$$w(\eta,\theta,t) = \sum_{j=1}^{N_w}\sum_{n=1}^{N}\left[W^{(j,n)}(\eta,\theta) f_{w,j,n}(t) + W_c{}^{(j,n)}(\eta,\theta) f_{w,j,n,c}(t)\right] \qquad (24)$$

These expansions respect exactly the simply supported boundary conditions.

The synchronicity is relaxed as for each mode $j$ and each component $(u, v, w)$ different time laws are allowed.

Mode shapes $U^{(j)}(\eta,\theta), V^{(j)}(\eta,\theta), W^{(j)}(\eta,\theta)$ are known functions expressed in terms of polynomials and harmonic functions, see Eqns. (16); the index *n* indicates the number of nodal diameters, the index *j* is used for ordering the modes (for each *n*) with increasing associated natural frequency. It is very interesting to note that, in the case of simply-simply supports, *j* is also the number of longitudinal half waves (number of nodal circumferences minus one), see Ref. [8].

The Lagrange equations for forced vibrations are expressed in the following form [8]

$$\frac{d}{dt}\left(\frac{\partial L}{\partial \dot{q}_i}\right) - \frac{\partial L}{\partial q_i} = Q_i \qquad \text{for } i\epsilon[1, N_{max}] \qquad (L = T_s - U_s) \qquad (25)$$

The modal coordinates are now ordered in a vector $\mathbf{q}(t) = [\ldots f_{u,j}, f_{v,j}, f_{w,j}, \ldots]$, $N_{max}$ depends on the number of modes considered in the expansions (24).

The generalized forces $Q_i$ are obtained by differentiation of the Rayleigh's dissipation function $F$ (14) and the virtual work done by external forces $W$ (13), in the form [8]

$$Q_i = -\frac{\partial F}{\partial \dot{q}_i} + \frac{\partial W}{\partial q_i} \qquad (26)$$

Expansions (24) are inserted into strain energy (11), kinetic energy (12), virtual work of the external forces (13) and damping forces (14).

Using Lagrange Eqns. (25), a set of nonlinear ordinary differential equations (ODE) is then obtained.

**Table 1.** Properties of stainless steel and nickel against coefficients of temperature.

| | stainless steel | | | nickel | | |
|---|---|---|---|---|---|---|
| | E | ν | ρ | E | ν | ρ |
| $P_0$ | $2.0 \times 10^{11}$ Nm$^{-2}$ | 0.326 | 8166 kgm$^{-3}$ | $2.2 \times 10^{11}$ Nm$^{-2}$ | 0.310 | 8900 kgm$^{-3}$ |
| $P_{-1}$ | 0 K | 0 K | 0 K | 0 K | 0 K | 0 K |
| $P_1$ | $3.1 \times 10^{-4}$ K$^{-1}$ | $-2.0 \times 10^{-4}$ K$^{-1}$ | 0 K$^{-1}$ | $-2.8 \times 10^{-4}$ K$^{-1}$ | 0 K$^{-1}$ | 0 K$^{-1}$ |
| $P_2$ | $-6.5 \times 10^{-7}$ K$^{-2}$ | $3.8 \times 10^{-7}$ K$^{-2}$ | 0 K$^{-2}$ | $-4.0 \times 10^{-9}$ K$^{-2}$ | 0 K$^{-2}$ | 0 K$^{-2}$ |
| $P_3$ | 0 K$^{-3}$ | 0 K$^{-3}$ | 0 K$^{-3}$ | 0 K$^{-3}$ | 0 K$^{-3}$ | 0 K$^{-3}$ |
| P | $2.1 \times 10^{11}$ Nm$^{-2}$ | 0.318 | 8166 kgm$^{-3}$ | $2.0 \times 10^{11}$ Nm$^{-2}$ | 0.310 | 8900 kgm$^{-3}$ |

## 5. NUMERICAL RESULTS

In this section, the nonlinear vibrations of functionally graded circular cylindrical shells with different mode shape expansions and geometries are considered.

Analyses are carried out on an FGM made of stainless steel and nickel.

FGM properties are graded in the thickness direction according to a volume fraction distribution, where $p$ is the power-law exponent.

The material properties, reported in Table 1, have been extracted from Ref. [2].

### Convergence Analysis

The convergence analysis is carried out on a simply supported cylindrical shell excited with a harmonic external force; the excitation frequency is close to the mode (*j*,*n*), where *j* is the number of longitudinal half waves and *n* is the number of nodal diameters.

The convergence is checked by adding suitable modes to the resonant one: asymmetric modes $(k \times j, s \times n)$ $k = 1{,}3$ $s = 1{,}2{,}3$ due to the presence of the quadratic and the cubic nonlinearities; axisymmetric modes $(k, 0)$ $k = 1{,}3{,}5{,}7$ due to the quadratic nonlinearities.

The analysis is then developed by introducing a different number of asymmetric and axisymmetric modes in the expansions (24), see also Tab. 2.

The FGM cylindrical shell is excited by means of an external modally distributed radial force $q_z = f_{1,6} \sin\eta \cos 6\theta \cos\Omega t$; the amplitude of excitation is $f_{1,6} = 0.0012h^2\varrho\omega_{1,6}^2$ and the frequency of excitation $\Omega$ is close to the mode $(1{,}6)$, $\Omega \cong \omega_{1,6}$.

The external forcing $f_{1,6}$ is normalized with respect to mass, acceleration and thickness; the damping ratio is equal to $\xi_{1,6} = 0.0005$.

**Table 2.** Asymmetric and axisymmetric modes inserted in the different nonlinear models.

| 6 dof model | 9 dof model | 12 dof model | 15 dof model | 18 dof model |
|---|---|---|---|---|
| mode (1,6) u, v, w | mode (1,6) u, v, w | mode (1,6) u, v, w | mode (1,6) u, v, w | mode (1,6) u, v, w |
| mode (1,12) v | mode (1,12) v | mode (3,6) u, v, w | mode (3,6) u, v, w | mode (3,6) u, v, w |
| mode (1,0) u, w | mode (3,12) v | mode (1,12) v | mode (1,12) v | mode (1,12) v |
| | mode (1,0) u, w | mode (3,12) v | mode (3,12) v | mode (3,12) v |
| | mode (3,0) u, w | mode (1,0) u, w | mode (1,18) v | mode (1,18) v |
| | | mode (3,0) u, w | mode (1,0) u, w | mode (3,18) v |
| | | | mode (3,0) u, w | mode (1,0) u, w |
| | | | mode (5,0) u, w | mode (3,0) u, w |
| | | | | mode (5,0) u, w |
| | | | | mode (7,0) u, w |

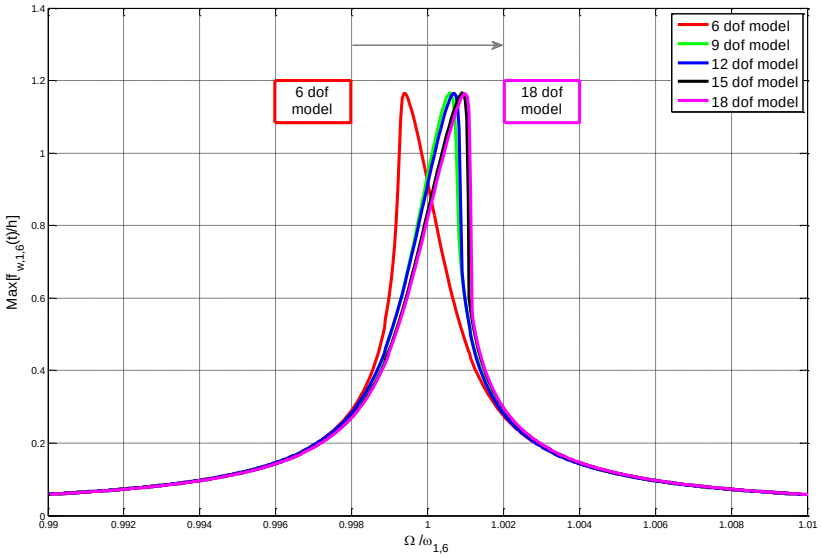


**Figure 2.** Convergence analysis. Nonlinear amplitude-frequency curves. Simply supported FGM circular cylindrical shell ($h/R$ = 0.002, $L/R$ = 20, $p$ = 1). "–", 6 dof model; "–", 9 dof model; "–", 12 dof model; "–", 15 dof model; "–", 18 dof model.

In the following, amplitude-frequency curves of the modal coordinates of the shell will be presented; the modal amplitudes are normalized with respect to the thickness $h$ of the shell and represented vs. the normalized frequency; for example, in representing the radial amplitude of mode (1,6), the maximum amplitude of $f_{w,1,6}(t)/h$ is represented vs. $\Omega/\omega_{1,6}$.

In Figure 2, amplitude-frequency curves of a simply supported FGM shell are shown ($h/R$ = 0.002, $L/R$ = 20, $p$ = 1, the shell is very thin and long), different expansions are compared. The 6 dof model (Table 2) gives a softening nonlinear behaviour, conversely, the higher-order expansions converge to a hardening nonlinear behaviour; higher order models (dof from 9 to 18) behave quite similarly; this means that the smallest expansion able to predict the dynamics with acceptable accuracy is 9 dof model (Table 2). The main weakness of the 6 dof expansion is the insufficient number of axisymmetric modes, which are very important for properly modelling the circumferential stretching during the vibration. It is to note that the shell is very thin, so the hardening behaviour is expected to occur (see e.g. Ref. [7]).

In Figure 3, a moderately thick and long FGM shell is analysed ($h/R$ = 0.025, $L/R$ = 20, $p$ = 1), the amplitude-frequency curves are obtained with the expansions of Table 2. Similar to the case of very thin FGM shell of Figure 2, the 6 dof model, with an insufficient number of axisymmetric modes, is clearly inaccurate; indeed, for this kind of FGM shell the correct behaviour is softening.

In Figure 4, a thick FGM shell is studied ($h/R$ = 0.050, $L/R$ = 20, $p$ = 1), the expected behaviour is hardening: the 6 dof model (Table 2) is inaccurate, similar to previous cases.

From the convergence analysis, one can claim that the 9 dof model gives satisfactory results with the minimal computational effort; therefore, in the following the 9 dof model of Table 2 will be used.

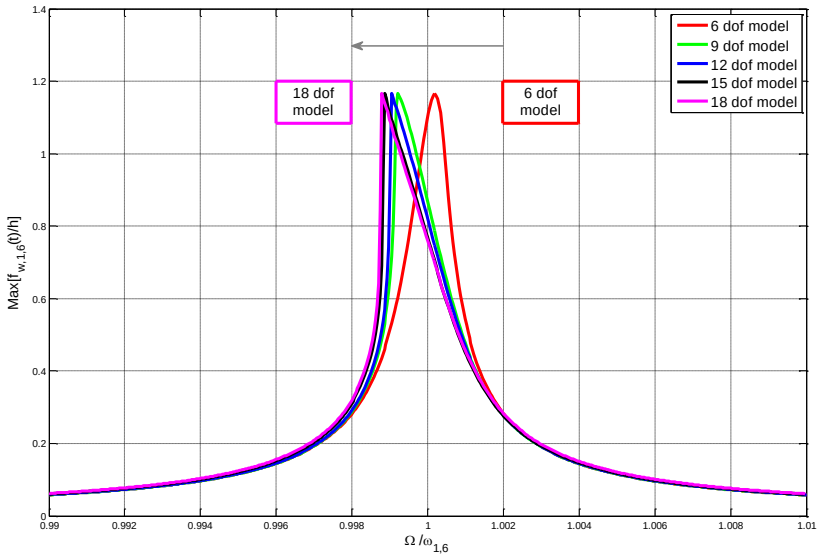


**Figure 3.** Convergence analysis. Nonlinear amplitude-frequency curves. Simply supported FGM circular cylindrical shell ($h/R$ = 0.025, $L/R$ = 20, $p$ = 1). "–", 6 dof model; "–", 9 dof model; "–", 12 dof model; "–", 15 dof model; "–", 18 dof model.

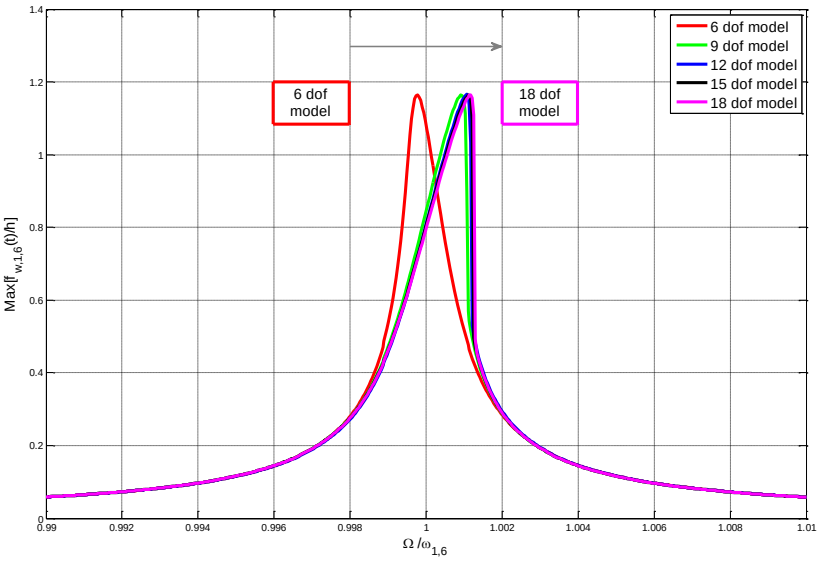


**Figure 4.** Convergence analysis. Nonlinear amplitude-frequency curves. Simply supported FGM circular cylindrical shell ($h/R$ = 0.050, $L/R$ = 20, $p$ = 1). "–", 6 dof model; "–", 9 dof model; "–", 12 dof model; "–", 15 dof model; "–", 18 dof model.

The previous considerations suggest the following 9 dof model be used for studying a generic resonant mode $(j, n)$:

- modes $(j, n), (1,0), (3,0)$ for the longitudinal displacement field $u$
- modes $(j, n), (j, 2n), \ (3j, 2n)$ for the circumferential displacement field $v$
- modes $(j, n), (1,0), (3,0)$ for the radial displacement field $w$.

After selecting such modes, each expansion present in Eqns. $(24)$ is then reduced to a three-terms modal expansion; the resulting nonlinear system has 9 dof.

**Companion mode participation**

In this section, the effect of the companion mode participation (Eqns. 24) on the nonlinear response is analysed.

The participation of both driven and companion modes gives a pure travelling wave response, moving circumferentially around the shell, when the time phase shift between two conjugate modal coordinates (e.g., $f_{w,1,6}(t)$ and $f_{w,1,6,c}(t)$) is $\pi/2$.

In Figure 5(a), the amplitude-frequency curve with the companion mode participation is presented ($h/R = 0.025$, $L/R = 20$, $p = 1$, mode (1,6)) using a 14 dof model (this expansion corresponds to the 9 dof model without the companion modes, where the same number of axisymmetric modes is considered).

The response $f_{w,1,6}(t)$ with the companion mode participation, solid blue line of Figure 5(a), is very similar to the response without the companion mode participation, dashed black line, see Figure 3.

Taking into account the companion mode, Figure 5(b), does not produce any variation except for a small region close to the resonance ($0.9996 < \Omega/\omega_{1,6} < 0.9999$), where the companion mode is excited by means of a 1:1 internal resonance.

It is worthwhile to stress that the modal excitation does not excite directly the companion mode; therefore, the internal resonance mechanism induces an energy transfer between the two conjugate (and linearly uncoupled) modes.

In Figure 6, the time histories of the driven mode (1,6), blue line, and companion mode, red line, for $\Omega/\omega_{1,6} = 0.9998$ are presented; the companion mode is initially not active, then an energy transfer takes place, the amplitude of the driven mode decreases and eventually the companion mode is excited.

In Figure 7, enlarged view of Figure 6, a time phase shift between the two modal coordinates (conjugate modes) close to $\pi/2$ is present; therefore, a travelling wave takes place.

It is worthwhile to stress that, even though the nonlinearity of the system is not strong, the onset of a travelling wave implies that the response of the shell is completely different with respect to a linear model.

In Figure 8, the spectrum of the time histories of Figure 6 is shown: the last part of the time history is considered, i.e., the transient dynamics are cut out.

The spectrum presents four spikes, one driven harmonic and three super harmonics of order two, three and four, respectively: this confirms the presence and the importance of quadratic and cubic nonlinearities.

## 6. CONCLUSIONS

In this paper, the nonlinear vibrations of FGM circular cylindrical shells are analysed; the Sanders-Koiter theory is applied to model the nonlinear dynamics of the system in the case of finite amplitude of vibration.

(a) (b)

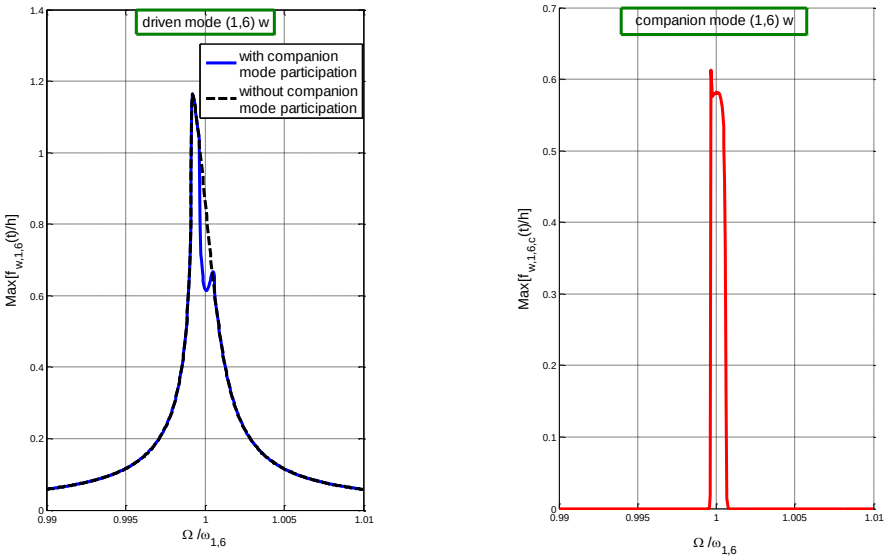


**Figure 5.** Amplitude-frequency curves of the FGM shell ($h/R$ = 0.025, $L/R$ = 20, $p$ = 1). 14 dof model. (a) "– –", driven mode (1,6) $w$ without companion mode participation; "–", driven mode (1,6) $w$ with companion mode participation. (b) Companion mode (1,6) $w$.

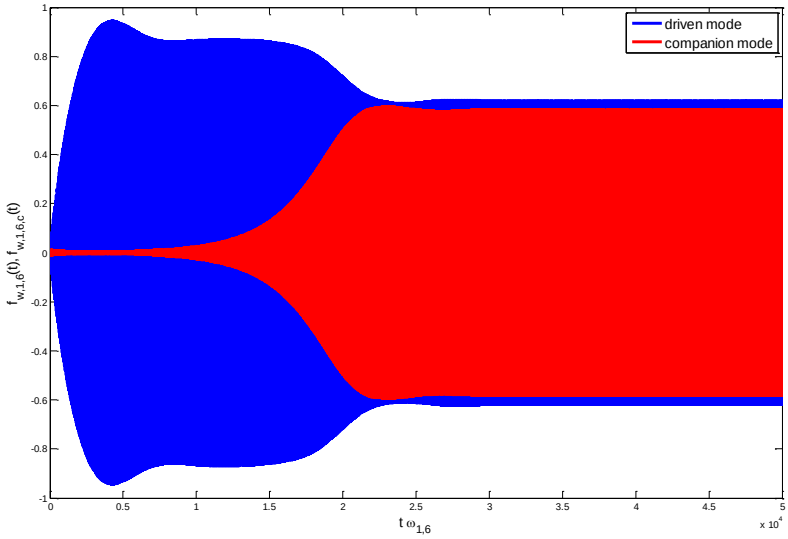


**Figure 6.** Time histories of the shell ($h/R$ = 0.025, $L/R$ = 20, $p$ = 1), transient included. "–", driven mode (1,6) $w$ with companion mode participation; "–", companion mode (1,6) $w$.

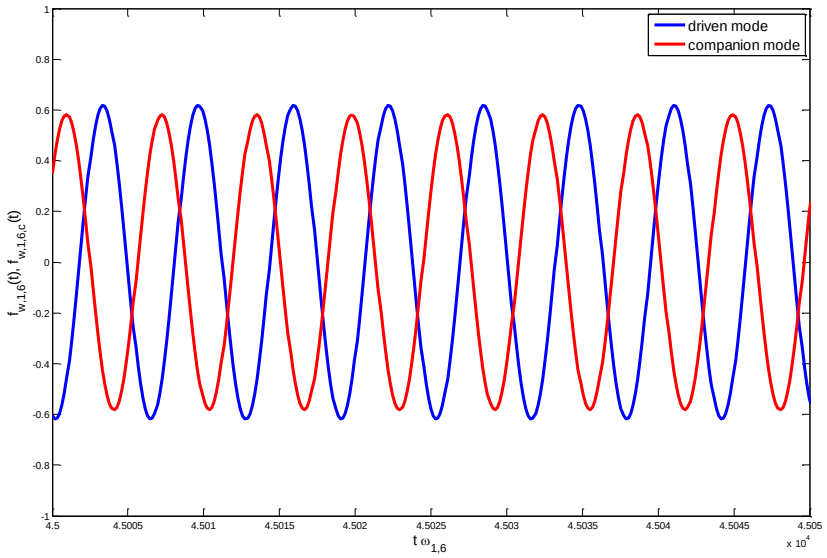


**Figure 7.** Time histories of the FGM shell ($h/R$ = 0.025, $L/R$ = 20, $p$ = 1), steady state. "–", driven mode (1,6) $w$ with companion mode participation; "–", companion mode (1,6) $w$.

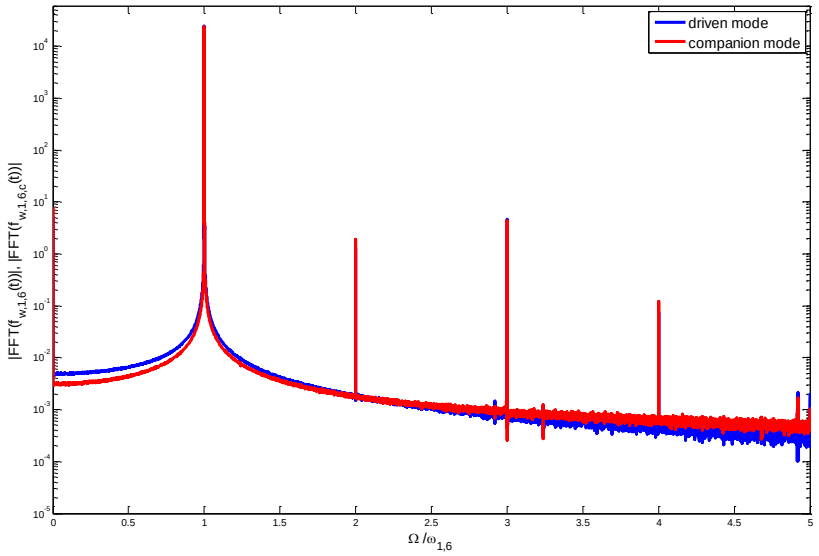


**Figure 8.** Spectrum of the time histories of the FGM shell ($h/R$ = 0.025, $L/R$ = 20, $p$ = 1), transient removed. "–", driven mode (1, 6) $w$ with companion mode participation; "–", companion mode (1, 6) $w$.

The functionally graded material is made of a uniform distribution of stainless steel and nickel, and the material properties are graded in the thickness direction, according to a volume fraction power-law distribution.

Numerical analyses are carried out in order to characterize the nonlinear response when the shell is subjected to a harmonic external load.

A convergence analysis is carried out by introducing in longitudinal, circumferential and radial displacement fields a different number of asymmetric and axisymmetric modes.

The fundamental role of the axisymmetric modes is confirmed, and the role of the higher-order asymmetric modes is clarified in order to obtain the actual character of nonlinearity.

An interesting result of the present study regards the predictions obtained with low-order expansions.

It is well known in literature that small expansions could lead to hardening behaviours when the actual shell response is softening.

Here we have found that when shells having actual hardening response are simulated with an insufficient expansion, their behaviour could appear spuriously softening.

The effect of the companion mode participation on the nonlinear response of the shells is analysed.

Both driven and companion modes are considered allowing for the travelling-wave response of the shell; amplitude-frequency curves with companion mode participation are obtained.

It is worthwhile to stress that, even though the nonlinearity of the system is weak, close to the resonance of asymmetric modes the onset of a travelling wave in the circumferential direction is possible.

This is a macroscopic effect of the weak nonlinearity that cannot be predicted with the linear models.

## REFERENCES


[1] Technical Report, Japanese Government, 1987. Research on the Basic Technology for the Development of Functionally Gradient Materials for Relaxation of Thermal-stress. Science and Technology Agency of Japanese Government.

[2] Loy CT, Lam KY, and Reddy JN, 1999. "Vibration of functionally graded cylindrical shells". *International Journal of Mechanical Sciences,* **41**, pp. 309–324.

[3] Pradhan SC, Loy CT, Lam KY, and Reddy JN, 2000. "Vibration characteristics of functionally graded cylindrical shells under various boundary conditions". *Applied Acoustics,* **61**, pp. 111–129.

[4] Leissa AW, 1973. *Vibrations of Shells*. Government Printing Office, Washington DC.

[5] Yamaki N, 1984. *Elastic Stability of Circular Cylindrical Shells*. North-Holland, Amsterdam.

[6] Amabili M, 2008. *Nonlinear Vibrations and Stability of Shells and Plates*. Cambridge University Press, New York.

[7] Pellicano F, 2007. "Vibrations of circular cylindrical shells: Theory and experiments". *Journal of Sound and Vibration,* **303**, pp. 154–170.

[8] Strozzi M, Pellicano F, 2013. "Nonlinear vibrations of functionally graded cylindrical shells". *Thin-Walled Structures,* **67**, pp. 63–77.